Available online at www.sciencedirect.com
ScienceDirect
Journal of Power Sources 174 (2007) 916–920
JOURNAL OF POWER SOURCES
www.elsevier.com/locate/jpowsour

Short communication

Studies of the electrochemical performance of Sn–Sb alloy prepared by solid-state reduction

Hailei Zhao [a,b,*], Chaoli Yin [a], Hong Guo [a], Jianchao He [a], Weihua Qiu [a,b], Yue Li [a]

[a] *Department of Inorganic Nonmetallic Materials, University of Science and Technology Beijing, Beijing 100083, China*
[b] *Beijing Key Lab of Advanced Energy Material and Technology, Beijing 100083, China*

Available online 28 June 2007

Abstract

The effects of particle size, chemical composition and cycling potential range on the electrochemical properties of micro-sized Sn–Sb electrodes were investigated in terms of initial irreversible capacity, rate-capability and cycling stability. Large particle sized SnSb electrode shows a low initial irreversible capacity and a relatively good cyclic performance when charged/discharged at 100 mAh g^{-1} due to the low specific surface area and loose structural characteristics of SnSb particles. When charged and discharged at high current density, large particle sized SnSb electrode displays a fast capacity fading compared to the small sized one due to the long diffusion distance of Li-ions. The Sn/Sb ratio has effect on the cycling stability of electrodes. Sn-riched and Sb-riched Sn–Sb electrodes exhibit fast capacity decline while sample with pure SnSb intermetallic phase shows a relatively good cycling stability. To increase the lower limit of cycling potential range cannot improve the cyclic performance while to decrease the upper limit to 0.8 V can control the cycling stability of SnSb electrode significantly. The Sb component is considered to be the main cause of the capacity fading of Sn–Sb electrode.

Keywords: Sn–Sb alloy; Electrochemical properties; Anode; Li-ion batteries

1. Introduction

Lithium storage alloys/intermetallics have been frequently proposed as alternatives to carbonaceous anode materials due to their very high Li packing density and hence high electrochemical capacity [1–3]. However, the higher Li packing density leads to a large volume change on Li uptake and removal, which easily causes anode cracking or pulverization, and thus affecting the cycling performance of electrode [4,5]. This can be improved by employing nano-sized active material [1,6] or by limiting the cycling potential range [7–9]. Unfortunately, the former usually results in a high initial irreversible capacity owing to its very high specific surface area, and in the latter cases the better cycling stability is achieved at the expense of capacity.

In order to minimize the mechanical stress in lithium alloy electrodes caused by the volume change during cycling, an effective strategy is to disperse active component that can alloy with lithium in different inert components, such as inert metal (V, Cu, Fe, Ni, etc.) [10–13] and plastic mixed-conducting materials [14]. The inert component can buffer the large volume change produced by the active component during cycling, and thus increase the mechanical stability of alloy electrode. The combination of two active elements, they alloy with lithium at different potentials, can also realize the excellent cycleability of electrode. The representative examples are SnSb and InSb [4,15]. Because the lithiation and delithiation of the two active components occur at different potentials, the unreacted phase can accommodate the mechanical strain yielded by the reacted phase, and hence make the volume change of the whole electrode take place much smoothly. On the other hand, this kind of alloys allows the electrode to keep at a high capacity, as both elements are capable of alloying with lithium.

Initial irreversible capacity for anode is a crucial factor in real batteries as it will consume the cathode material as compensation. The high initial irreversible capacity is one of the main problems for alloy anodes, which impede their commercialization. Decreasing the initial capacity loss may promote the practical use of alloy anode in high energy Li-ion batteries. In this contribution, micro-sized Sn–Sb powders were synthesized via solid-state reduction from SnO_2 and Sb_2O_3 with the aim to diminish the surface impurity of Sn–Sb particles and thus decrease the initial irreversible capacity. The effect of particle

* Corresponding author. Tel.: +86 10 62334863; fax: +86 10 62332570.
E-mail address: hlzhao@mater.ustb.edu.cn (H. Zhao).

0378-7753/$ – see front matter © 2007 Elsevier B.V. All rights reserved.
doi:10.1016/j.jpowsour.2007.06.143

size on the initial irreversible capacity, and the effects of the chemical composition of active material and the cut-off voltages of charge/discharge cycling on the cycling performance of micro-sized Sn–Sb electrode were investigated.

2. Experimental

Micro-sized powders with Sn/Sb ratios of 2:1, 1:1 and 1:2, labeled as Sn/SnSb, SnSb and Sb/SnSb, respectively, were synthesized by solid-state reaction from SnO_2, Sb_2O_3 and carbon in argon atmosphere. The starting materials were mixed by ball-milling in ethanol for 8 h, followed by drying in a 105 °C-oven. The homogeneously mixed powders were placed in a quartz glass crucible and calcined at 850 °C in argon atmosphere for different time in a Al_2O_3-tube furnace. Different sized Sn–Sb powders are obtained by controlling the reaction time from 2 to 6 h. XRD was used to identify the phase composition and SEM was employed to characterize the particle morphology of Sn–Sb powders.

Sn–Sb electrodes were prepared by pasting a slurry consisting of 75 wt% Sn–Sb active materials, 15 wt% carbon black and 10 wt% polyvinylidene fluoride (PVdF) dispersed in *N*-methyl-2-pyrrolidone onto a Cu foil. After pre-drying at 60 °C, the electrodes were pressed and rigorously dried in dynamic vacuum at 130 °C overnight. Half-cell studies were performed in laboratory-type cells with excessive organic electrolyte (1 M $LiPF_6$/EC + DMC, 1:1, v/v) and metallic Li as counter electrode. Cycling tests were carried out at different current densities of 50, 100 and 200 mA g^{-1} with a cut-off of 0.01 V/1.2 V versus Li/Li^+. In order to examine the charge and discharge depth effect on the cycling performance, Sn–Sb electrodes were cycled at different voltage ranges. Cyclic voltammograms (CVs) was recorded between 1.6 and 0.01 V with scan rate of 0.05 mV s^{-1}.

3. Results and discussion

Three kinds of Sn–Sb powders with average particle size of 10 μm was synthesized at 850 °C for 2 h, in which Sn/SnSb, SnSb and Sb/SnSb were identified by XRD, respectively. Fig. 1 shows the XRD patterns of these three Sn–Sb powders. No peaks designable to corresponding oxides are detected, indicating that SnO_2 and Sb_2O_3 have been reduced completely. The high peak intensities suggest the high crystallinity of synthesized Sn–Sb powders. Carbon analysis reveals that a certain amount of carbon (3–5 wt%) remains in the Sn–Sb powders. This should be beneficial to the cycling stability of Sn–Sb alloy anode as carbon can not only enhance the electronic conduction of electrode but also buffer the volume change caused by the lithiation and delithiation of Sn–Sb active materials. SEM observation discloses a spherical morphology of the synthesized Sn–Sb powders, as shown in Figs. 2 and 3. A close inspection reveals that the spherical particles of Sn–Sb powders present a loose and polycrystalline structure [16] rather than a dense one.

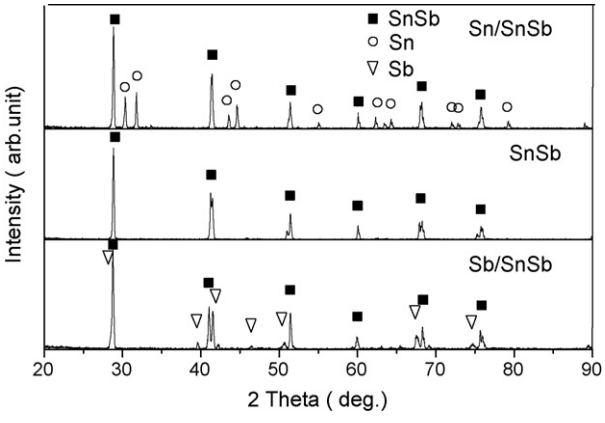

Fig. 1. XRD patterns of Sn–Sb powders synthesized at 850 °C for 2 h by solid-state reduction.

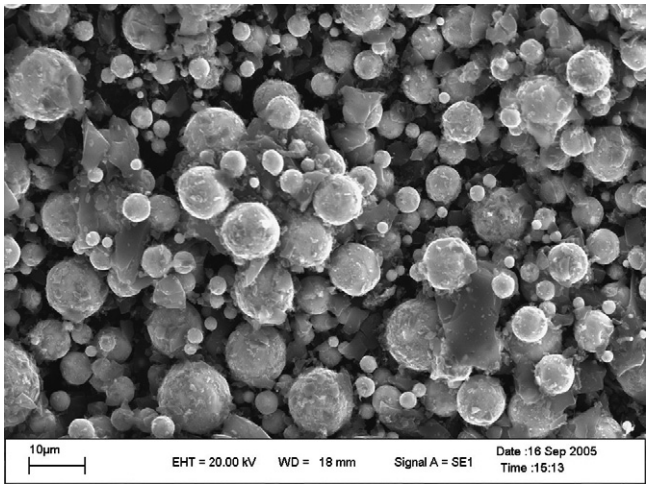

Fig. 2. SEM image of sample SnSb synthesized at 850 °C for 2 h.

3.1. Particle size effect

In order to make an insight into the effect of particle size on the electrochemical performance of alloy electrode, sample SnSb was calcined at 850 °C for 2 and 6 h, respectively. The 2 h-sample shows an average particle size of ca. 8 μm while the 6 h-sample presents an average particle size of 20 μm, as illustrated

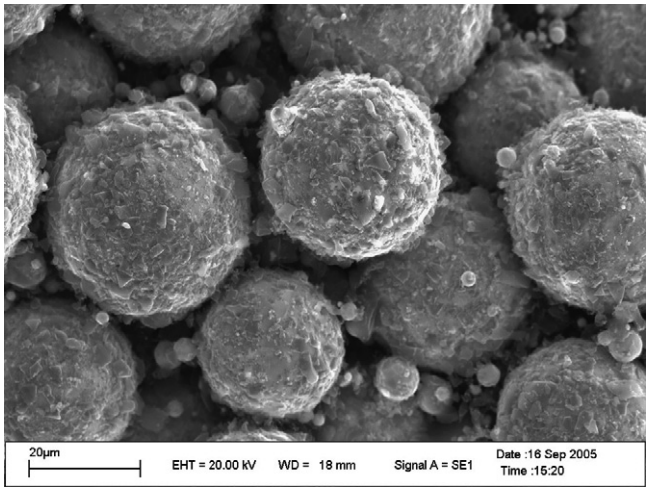

Fig. 3. SEM image of sample SnSb synthesized at 850 °C for 6 h.

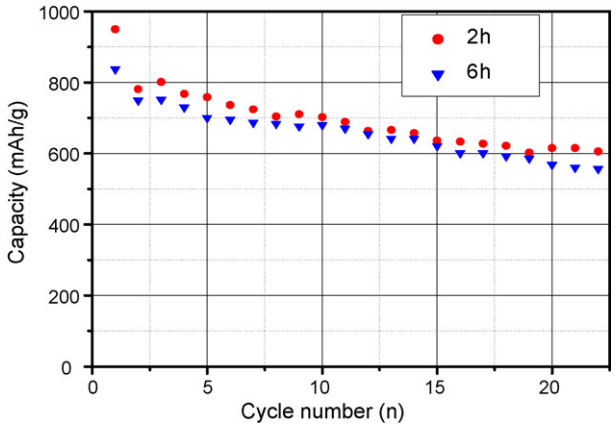

Fig. 4. Cycling performance of SnSb samples synthesized at 850 °C for 2 and 6 h, respectively. The current density is 100 mA g^{-1}.

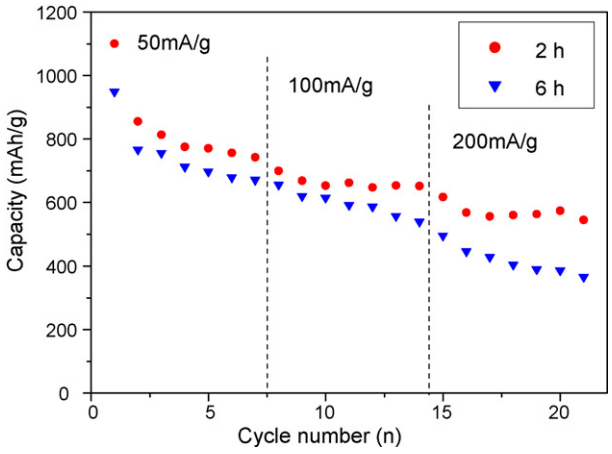

Fig. 5. Specific capacities of 2- and 6 h-samples as a function of cycle number. The charge and discharge current density is 50 mA g^{-1} for the first seven cycles, and 100 and 200 mA g^{-1} for the second and third seven cycles, respectively.

in Figs. 2 and 3, respectively. Prolonging the holding time at 850 °C can increase the particle size of SnSb sample remarkably and, at the same time, make the particle size distribution more narrow and homogeneous.

The cycling performance of the two samples with different particle sizes is shown in Fig. 4. The 2 h-sample shows an initial irreversible capacity of 165 mAh g^{-1} while the 6 h-sample displays 86 mAh g^{-1}, indicating that the particle size has strong impact on the initial irreversible capacity of SnSb electrode. BET analysis gives a specific surface area of 85.504 m^2 g^{-1} for 2 h-powders and of 23.846 m^2 g^{-1} for 6 h-powders. Large particle size corresponds to low specific surface area and thus low surface contaminant, which is produced during the electrode preparation process and is considered to be the main reason of the initial irreversible capacities. Therefore, increasing the particle size of active powder is apparently beneficial to the decrease of initial capacity loss. It is worth to note that the initial irreversible capacities of the two investigated samples (2 and 6 h-samples) are both significantly lower than the most reported values of nano-sized SnSb anode [5,17,18].

The two samples show high specific capacities on second cycles, 780 mAh g^{-1} for 2 h-sample and 750 mAh g^{-1} for 6 h-sample, but they degrade gradually with charge and discharge cycling. Nevertheless, they retain ca. 600 mAh g^{-1} after 20 cycles. Usually, the micro-sized alloy electrode shows fast capacity degradation upon cycling due to the large absolute volume change of single particle, which will result in the crack or pulverization of single particle or even electrode [19]. The relatively good cycling stability of synthesized SnSb powders with micro-sized particles can be attributed to the loose structure feature and the polycrystalline characteristics of the synthesized SnSb particles (Fig. 3). The single spherical particle shown outwardly is practically an aggregate with many small particles inside, thus the space possibly existing inside the spherical particles can accommodate the volume change and release the stress generated during the lithiation and delithiation of SnSb electrode. As expected, the two samples show similar cycling performance due to their similar structure features, although the particles of 6 h-sample is two to three times larger than that of 2 h-sample.

The rate-capability of two samples was investigated at different current densities. The results are shown in Fig. 5 (the data for 2 h-sample has ever been published in [20], which is listed here just for comparison). The electrodes were charged and discharged at 50 mA g^{-1} for first seven cycles and then followed by 100 and 200 mA g^{-1} for second and third seven cycles, respectively. The two samples have similar cycling performance at low current density, while 6 h-sample shows a relatively faster capacity fading at high current density when compared to 2 h-sample. With the current density increasing, the capacity difference between two samples increases, indicating that 6 h-sample with large particle size has a slow kinetic process. The comparatively long diffusion distance of Li-ions in 6 h-sample should be accountable for this phenomenon. It is apparently that large particle size of the synthesized SnSb active material is unfavorable for the rate-capability of electrode although it shows a low initial capacity loss.

3.2. *Composition effect*

The cyclic performance of samples Sn/SnSb, SnSb and Sb/SnSb synthesized at 850 °C for 2 h are shown in Fig. 6. Compared to Sn/SnSb and Sb/SnSb composite samples, the pure intermetallic SnSb sample exhibits a relatively good cycling stability. At the first several cycles, Sn/SnSb shows a similar cycling behavior with SnSb, a good cycling stability is maintained. With the cycle going on, however, a fast capacity decline is observed for sample Sn/SnSb. On the other hand, Sb/SnSb shows fast capacity degradation even at the initial stage, suggesting that Sb component may cause more irreversible capacity during the lithiation and delithiation process.

Because the lithiation and delithiation potentials are different for Sn and Sb components, the volume change of Sn–Sb electrodes will occur in a multi-step manner, as reflected in Fig. 7. Peaks A and A' represents the lithiation and delithiation process of component Sb, while peak pairs of B–B', C–C' and D–D' correspond to the potential dependent lithiation and delithiation process of component Sn. CV plots demonstrate

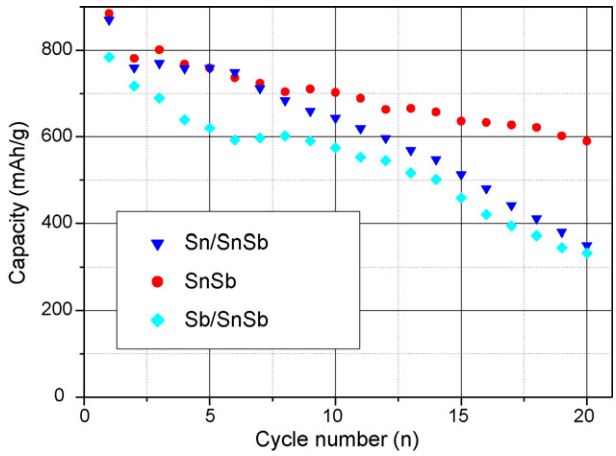

Fig. 6. Cyclic performance of samples Sn/SnSb, SnSb and Sb/SnSb synthesized at 850 °C for 2 h. The current density is 100 mA g^{-1}.

that samples Sn/SnSb and SnSb show a relatively homogeneous volume change, which has been divided to take place at different potentials, as demonstrated in Fig. 7(a and b). Contrary, Sb-riched sample (Sb/SnSb) exhibits a high capacity at potential corresponding to the lithiation and delithiation of Sb due to its high Sb content, as shown in Fig. 7(c), which will cause a large volume change at that potential. More volume change occurring suddenly at the same potential may cause the particle cracking and thus leading to a fading performance, as reflected

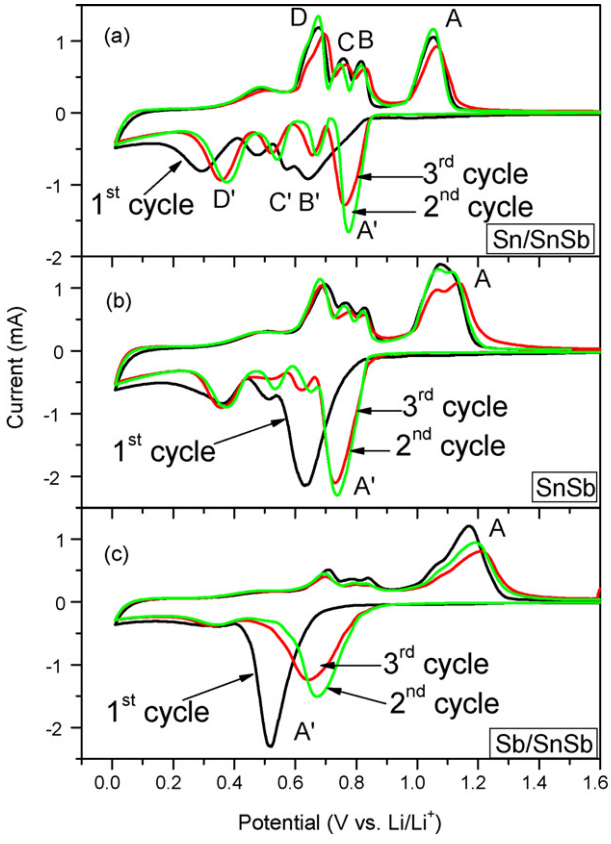

Fig. 7. Cyclic voltammograms for Sn/SnSb (a), SnSb (b) and Sb/SnSb (c) obtained at 0.05 mV s^{-1} between 0.01 and 1.6 V vs. Li/Li^+.

in Fig. 6. The fast capacity fading of sample Sn/SnSb may due to the phase transformation and the re-aggregation of Sn particles during cycling process [21,22].

The potential difference between the anodic and cathodic peaks can reflect the polarization state of the electrode. For peak pair of A–A', the potential difference is 0.33, 0.35 and 0.40 V for samples Sn/SnSb, SnSb and Sb/SnSb, respectively, showing that the polarization of electrode is increased with the increased content of Sb component. This is another reason that Sb/SnSb electrode shows a lower specific capacity compared to Sn/SnSb and SnSb electrodes.

3.3. Cycling potential range effect

To limit the cycling potential range of electrode may have effect on the cycling stability of Sn–Sb electrodes. Sample SnSb was cycled in different potential ranges to limit the lithiation and delithiation process of some component. The results are shown in Fig. 8. To increase the lower limits of cycling potential range cannot improve the cycling stability of SnSb electrode, while to decrease the upper limits to 0.8 V can control the capacity decline significantly, although a relatively low specific capacity is remained. According to the charge and discharge curves of SnSb electrode, as illustrated in Fig. 9, increasing the lower limit of cycling potential range to 0.3 V will sacrifice some capacity coming from Sn component, while lowering the upper limit of cycling potential range down to 0.8 V will lead to the impossibility of Li-ion extraction from Sb component. In potential range 0.3–1.2 V, Sb and partial Sn components are active, while only Sn component is active when cycled in 0.01–0.8 V. The good cycling stability of SnSb electrode cycled in 0.01–0.8 V and the fast capacity decline feature of SnSb electrode cycled in 0.3–1.2 V suggest that the capacity fading of SnSb electrode mainly comes from Sb component rather than Sn component, in other words, Sb component, compared to Sn component, has high irreversibility against the lithiation and delithiation process.

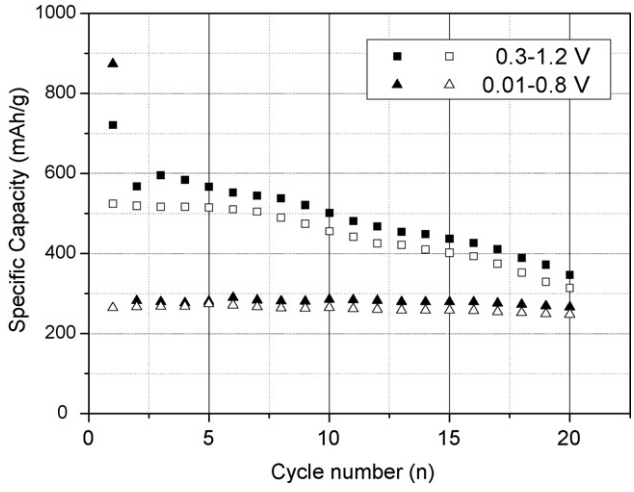

Fig. 8. Specific capacity of sample SnSb as a function of cycle number. The cut-off voltage is 0.3–1.2 V and 0.01–0.8 V, respectively. The current density is 100 mA g^{-1}. The solid symbols represent the lithiation process while the hollow symbols represent the delithiation process.

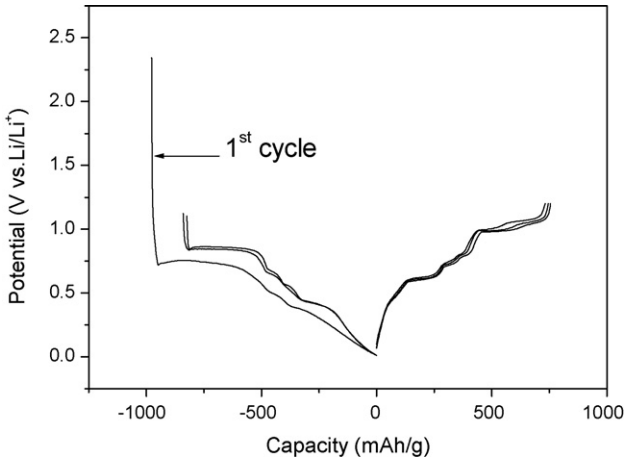

Fig. 9. Charge/discharge profiles of SnSb sample synthesized at 850 °C for 2 h.

An interesting phenomenon needs to note that the irreversible capacity (the difference between charge and discharge capacity) is high for SnSb electrode when cycled in 0.3–1.2 V, but is very low when cycled in 0.01–0.8 V. The reason remains to be investigated further. The initial lithiation capacity of SnSb electrode is very high when cycled in 0.0–0.8 V, ca. 880 mAh g^{-1}. From second cycle, the capacity is maintained stably at ca. 280 mAh g^{-1}. The relatively lower initial lithiaition potential (<0.8 V) and higher delithiation potential (ca. 1.0 V) of Sb component will result in that Li-ions can not be extracted from initially lithiated Sb (Li_3Sb) when the upper voltage limit is set as 0.8 V. From second cycle, Li_3Sb will play as a buffer in SnSb electrode to accommodate the volume change caused by Sn component during charge and discharge process leading to a stable cycling performance of electrode.

4. Conclusions

Micro-sized SnSb powders with different chemical compositions and different particle sizes were synthesized via solid-state reduction. The particle size has a strong impact on the initial irreversible capacity of Sn–Sb electrode. Due to its low specific surface area, SnSb powders with large particle size has less possibility to contact with oxygen in atmosphere and with electrolyte in the cell, leading to a lower surface contamination and less SEI film, which is considered to be the main reason of the initial irreversible capacity. The large particle sized SnSb powders, however, show a relatively poor rate-capability when compared with small particle sized SnSb powders. The Sn/Sb ratio also plays an important role in the cycling stability of Sn–Sb electrodes. Compared with Sn-riched and Sb-riched Sn–Sb powders, sample with pure SnSb intermetallic phase exhibits a good cycling stability. More volume change of electrode due to alloying and de-alloying of Sn–Sb with Li occurring suddenly at same potential is apparently unfavorable to the cycling performance of electrode. To limit the charge/discharge depth of SnSb electrode can alter the specific capacity and cycling stability of electrode. To increase the lower limits of cycling voltage range cannot improve the cycling stability of SnSb anode, whereas to decrease the upper limits to 0.8 V can control the capacity decline significantly, although a large amount of capacity is sacrificed. The experimental data suggest that Sb component is the main cause of the capacity fading for Sn–Sb electrode.

Acknowledgment

This research work was kindly supported by 863 Program of National High Technology Research Development Project of China (No. 2006AA03Z231) and National Natural Science Foundation of China (No. 50371007).

References

[1] M. Winter, J.O. Besenhard, Electrochim. Acta 45 (1999) 31–50.
[2] M. Wachtler, M. Winter, J.O. Besenhard, J. Power Sources 105 (2002) 151–160.
[3] X. Cheng, P. Shi, J. Alloys Compd. 391 (2005) 241–244.
[4] J. Yang, M. Wachter, J.O. Besenhardard, Electrochem. Solid State Lett. 2 (1999) 161–163.
[5] M. Wachtler, J.O. Besenhard, M. Winter, J. Power Sources 94 (2001) 189–193.
[6] J. Yang, M. Winter, J.O. Besenhard, Solid State Ionics 90 (1996) 281.
[7] J. Yang, Y. Takeda, N. Imanishi, et al., Solid State Ionics 135 (2000) 175–180.
[8] J.R. Owen, W.C. Maskell, B.C.H. Steele, T.S. Nielsen, O.T. Sorensen, Solid State Ionics 13 (1984) 329.
[9] W.C. Maskell, J.R. Owen, J. Electrochem. Soc. 132 (1985) 1602.
[10] H. Yoshinaga, A. Kawabata, Y. Xia, T. Sakai, J. Jpn. Soc. Powder Powder Metall. 49 (1) (2002) 37–43.
[11] D.G. Kim, H. Kim, H.J. Sohn, T. Kang, J. Power Sources 104 (2002) 221–225.
[12] O. Mao, R.A. Dunlap, J.R. Dahn, J. Electrochem. Soc. 146 (2) (1999) 405–413.
[13] H. Mukaibo, T. Momma, T. Osaka, J. Power Sources 146 (1–2) (2005) 457–463.
[14] X. Zhang, C. Wang, A.J. Appleby, F.E. Little, J. Power Sources 109 (2002) 136–141.
[15] J.T. Vaughey, C.S. Johnson, A.J. Kropf, R. Benedek, M.M. Thackeray, H. Tostmann, T. Sarakonsri, S. Hackney, L. Fransson, K. Edstrom, J.O. Thomas, J. Power Sources 97–98 (2001) 194–197.
[16] H. Zhao, D.H.L. Ng, Z. Lu, N. Ma, J. Alloys Compd. 395 (2005) 192–200.
[17] H. Mukaibo, T. Osaka, P. Reale, S. Panero, B. Scrosati, M. Wachtler, J. Power Sources 132 (2004) 225–228.
[18] I. Rom, M. Wachtler, I. Papst, M. Schmied, J.O. Besenhard, F. Hofer, M. Winter, Solid State Ionics 143 (2001) 329–336.
[19] J.O. Besenhard, M. Wachtler, M. Winter, R. Andreaus, I. Rom, W. Sitte, J. Power Sources 81–82 (1999) 268–272.
[20] H. Zhao, C. Yin, H. Guo, W. Qiu, Electrochem. Solid-State Lett. 9 (6) (2006) A281–A284.
[21] H. Li, X.J. Huang, L.Q. Chen, Z.G. Wu, Y. Liang, Electrochem. Solid-State Lett. 2 (1999) 547.
[22] Z.X. Liao, F.Z. Ma, J.H. Hu, Electrochem. Commun. 5 (2003) 657.